SEMARAK ILMU PUBLISHING

Semarak Engineering Journal

Journal homepage:
https://semarakilmu.my/index.php/sej/index
ISSN: 3036-0145



Thermal-Analysis-Guided Solution Treatment and Aging-Time Effects on Tensile Behavior and Bending Fatigue Life of Commercial AA6061 Aluminum Alloy

Faizal Safa[1], Nukman[2,*], Irsyadi Yani[2]

[1] Faculty of Engineering, Universitas Sriwijaya, Palembang, Sumatera Selatan, Indonesia
[2] Department of Mechanical Engineering, Faculty of Engineering, Universitas Sriwijaya, Indralaya, 30662, South Sumatra, Indonesia

ARTICLE INFO

Article history:
Received 6 September 2026
Received in revised form 13 October 2026
Accepted 10 November 2026
Available online 24 November 2026

Keywords:
Aluminum alloy 6061; Solution treatment; Artificial aging; Tensile properties; Bending fatigue.

ABSTRACT

This study investigated the effects of solution treatment and artificial aging duration on the tensile properties and bending fatigue life of commercial aluminum alloy 6061. Thermal analysis identified characteristic changes near 611 and 653 degrees Celsius, providing preliminary guidance for selecting the treatment temperature. Specimens were heated at 550 degrees Celsius for one hour, rapidly cooled in water, and subsequently aged at a nominal temperature of 150 degrees Celsius for three, five, and seven hours. Tensile testing revealed that the untreated material exhibited a yield strength of 190.03 megapascals, while the treated specimens showed lower values ranging from 111.27 to 129.01 megapascals. Differences in reported elongation measurements prevented a reliable assessment of changes in ductility. Bending fatigue testing demonstrated that the influence of aging duration varied across loading conditions. At the intermediate loading setting, specimens aged for seven hours achieved 3.04 million cycles, compared with 1.87 million cycles for untreated specimens, representing an increase of approximately 62.6 percent. However, this improvement was not consistently observed under other loading conditions. Overall, the findings indicate that aging duration influences fatigue performance without necessarily improving tensile strength. Further testing is required to confirm reproducibility and establish reliable relationships between treatment conditions and mechanical behavior.

1. Introduction

Aluminum alloys of the 6xxx series are widely employed in transportation and structural components because they combine low density, corrosion resistance, and useful formability. In applications subjected to repeated loading, however, conventional tensile properties alone do not characterize service performance. The properties of precipitation-hardenable AA6061 depend on its chemistry, initial temper, and thermal history [1], [2]. This dependence is especially relevant for

* *Corresponding author.*
E-mail address: nukman@ft.unsri.ac.id

https://doi.org/10.37934/sej.17.1.150163

commercially sourced material for which the original temper and processing history may not be fully documented.

The strengthening response of Al–Mg–Si alloys is associated with precipitation from a supersaturated solid solution through Guinier–Preston zones and metastable precipitates, particularly β″, before progressing toward coarser phases [3]. Solution treatment and quenching establish the starting condition for subsequent precipitation, whereas aging temperature and duration influence the final balance of strength and ductility. Studies of AA6061 and related 6xxx alloys report different responses in yield strength, tensile strength, and hardness as the aging schedule changes [2][8][9]. Interrupted or multistage aging has also been explored, but its benefits depend on both the alloy and the precise temperature–time pathway [10][11][12][13].

Selecting a solution treatment temperature also requires careful interpretation of thermal characterization. The solvus boundary concerns dissolution of precipitates in the solid state, while the solidus concerns the onset of liquid formation. Results for Al–Mg–Si systems indicate that actual dissolution behavior may differ from simplified phase-diagram predictions [4]. Under ICTAC terminology, thermogravimetry monitors mass change and differential thermal analysis monitors a sample–reference temperature difference [5]. Consequently, a TGA mass signal by itself is not evidence of melting onset. Thermal analysis of aluminum-containing materials further depends on processing conditions and oxidation behavior [6][7].

Recent investigations have connected solution treatment, precipitation evolution, and mechanical behavior in AA6061 [24][16][17][18][25]. Reports of melting ranges and thermal processing windows [19][20][21][22][23][26] provide useful context, although the thermal response of the present commercial stock should be interpreted on its own merits. Fatigue behavior is an additional, non-equivalent performance measure: prior work has documented sensitivity to precipitates, material condition, loading mode, and test parameters [14][15][27][28][29][30]. Therefore, an apparent strength increase should not be treated as proof of a longer fatigue life.

This study examines whether thermal-analysis-informed screening of a solution-treatment temperature, followed by three aging durations, provides a useful comparative framework for the tensile and displacement-controlled bending-fatigue responses of one commercial AA6061 stock. The contribution is a joint description of static and cyclic responses under the reported processing and test settings, not a new solutionizing mechanism or a demonstrated optimization of AA6061. Unlike conventional temperature selection based solely on a nominal alloy grade, the reported DTA event was considered as a stock-specific screening observation. However, without independent solvus, incipient-melting, and microstructural verification, the thermal-analysis-guided designation should not be interpreted as proof that 550 °C is optimal or that complete dissolution occurred.

2. Materials and Experimental Design

2.1 Material and Nominal Composition

The investigated material was commercially sourced AA6061 aluminum alloy in the as-received condition, designated as NHT in the experimental figures. The actual chemical composition and initial temper of the supplied material were not independently verified through chemical analysis or supplier certification. Accordingly, Table 1 presents the nominal chemical composition of AA6061 based on the cited reference [19], rather than experimentally measured values for the investigated batch. The unknown initial material condition, including potential effects of prior rolling, extrusion, and thermal processing, may influence the mechanical response of the as-received specimens and their subsequent response to heat treatment [21].

Table 1
Chemical composition of AA6061 (wt.%)

Element	Mg	Si	Cr	Mn	Ti	Cu	Zn	Fe	Al
Composition	0.80 - 1.2	0.40 - 0.8	0.04 - 0.35	0.15 max	0.15 max	0.15 - 0.40	0.25 max	0.7 max	Balance

2.2 Thermal Characterization and Selection of Solution-Treatment Temperature

Thermal characterization was performed using thermogravimetric and differential thermal analysis (TGA/DTA) to examine the thermal response of the commercially sourced AA6061 alloy. The resulting thermogram was used as a preliminary screening reference for selecting the solution-treatment temperature. The experimental selection of 550 °C was initially based on an empirical estimate corresponding to approximately 90% of the reported DTA event near 611 °C, together with consideration of published solution-treatment practices for AA6061 and related aluminum alloys [24][4][5][6][7][21][23][26].

However, the empirical calculation based on a Celsius temperature ratio does not constitute a thermodynamically valid criterion for selecting a solution-treatment temperature. Furthermore, a thermal event associated with the onset of melting cannot be directly interpreted as the solvus temperature or as evidence of complete Mg–Si precipitate dissolution. Therefore, the selected temperature of 550 °C was treated as an experimental processing condition informed by preliminary thermal observations and existing literature, rather than as a thermodynamically optimized solution-treatment temperature. The measured thermal response and its implications are presented in Sections 3.1 and 4.1, respectively.

2.3 Heat-Treatment Schedule

The AA6061 specimens were solution treated at 550 °C for 1 h, followed by immediate water quenching to room temperature. Subsequently, artificial aging was performed for three independent holding durations of 3, 5, and 7 h. Each aging duration represented a separate treatment condition rather than a successive or interrupted aging sequence.

As illustrated in Figure 1, the heat-treatment diagram indicates 120 °C as the minimum artificial-aging temperature, rather than the specific temperature applied to all experimental specimens. The mechanical testing results were reported for specimens designated 150-3, 150-5, and 150-7, corresponding to nominal artificial aging at 150 °C for 3, 5, and 7 h, respectively. Therefore, the 120 °C value shown in Figure 1 represents the lower temperature reference in the original heat-treatment diagram, whereas 150 °C denotes the nominal aging temperature associated with the investigated mechanical-test conditions. Confirmation of the actual furnace temperature from the original experimental records remains necessary to establish the precise thermal-treatment conditions.

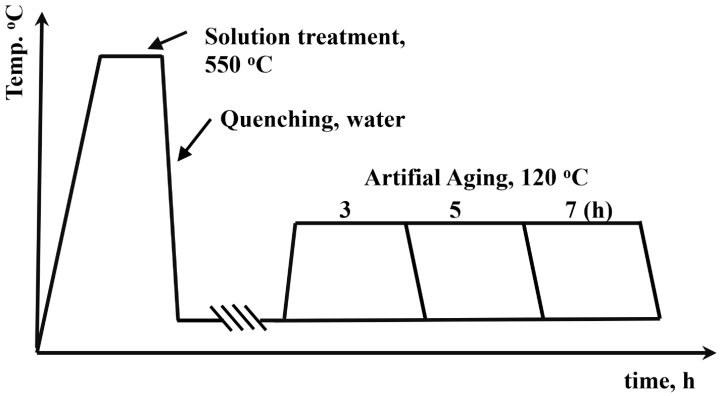

Fig. 1. Heat-treatment schedule of AA6061 specimens showing solution treatment at 550 °C for 1 h, water quenching, and artificial aging for 3, 5, and 7 h. The indicated 120 °C represents the minimum artificial-aging temperature, while the mechanical-test conditions are nominally designated at 150 °C

2.4 Tensile Testing

Tensile specimens were prepared according to ASTM E8M-11 and tested using a Gotech GT-7000 universal testing machine. The specimen geometry is presented in Figure 2. The tensile response was used to obtain the reported yield stress, ultimate tensile stress, and elongation values for the as-received and artificially aged conditions.

The available experimental records do not establish the number of independent specimens tested under each condition, whether the reported curves represent individual tests or averaged responses, or the procedures used to determine strain and elongation. In addition, the yield-stress determination method, including the possible application of a 0.2% offset criterion, was not documented. Consequently, the reported tensile properties are treated as individual condition-level observations rather than statistically established mean values. Standard deviations, confidence intervals, and statistical significance tests were not calculated because the necessary specimen-level measurements were unavailable.

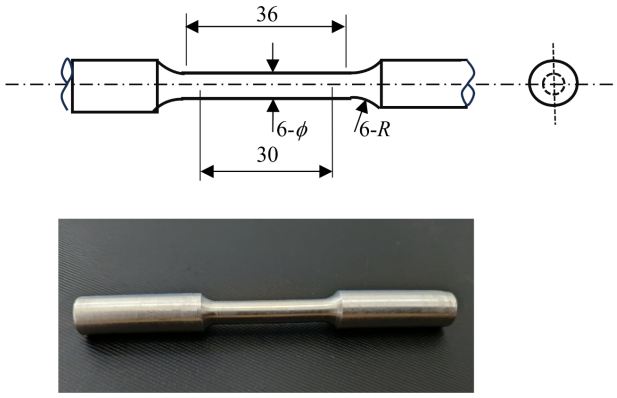

Fig. 2. Geometry and photograph of the tensile specimen used for mechanical testing.

2.5 Cantilever-Bending Fatigue Testing

Bending-fatigue tests were performed using an FTS-4 Repeated Torsion & Bending Fatigue Testing Machine in a cantilever clamping configuration, with the original experimental procedure referring to JIS Z 2273. The specimen geometry is illustrated in Figure 3. Tests were conducted at nominal machine-angle settings of 4°, 5°, and 6°, corresponding to reported imposed tip displacements of 2.8, 3.5, and 4.2 mm, respectively. The fatigue life was expressed as the number of cycles to failure under each imposed-displacement condition.

The nominal machine-angle settings were used to define the experimental loading conditions and were not independently calibrated as equivalent bending-stress amplitudes. Although the nominal bending stress at the critical section can be expressed using the elastic beam relationship,

$$\sigma = Mc/I \quad (1)$$

where σ is the nominal bending stress, M is the bending moment, c is the distance from the neutral axis to the outermost fiber, and (I) is the second moment of area, its reliable determination requires verified applied forces, specimen geometry, and fixture boundary conditions. For a cantilever subjected to an end force (F) at a distance (L) from the critical section, the nominal bending moment is given by

$$M = FL \quad (2)$$

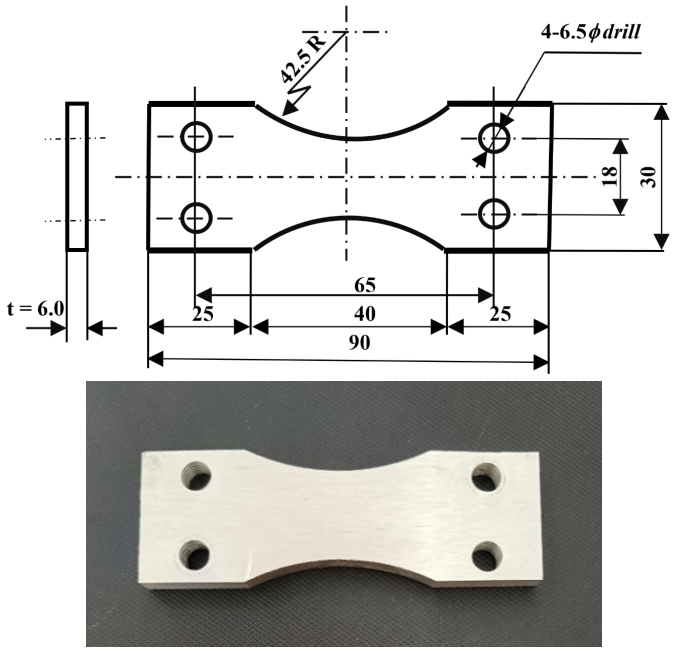

Fig. 3. Geometry and photograph of the specimen used for cantilever-bending fatigue testing

3. Results

3.1 Thermal Response and Selected Processing Window

Figure 4 presents the thermogravimetric and differential thermal analysis (TGA/DTA) response of the commercially sourced AA6061 aluminum alloy. The reported DTA thermogram exhibits two characteristic thermal features at approximately 611 °C and 653.3 °C, originally assigned to the onset

and completion of melting, respectively. The selected solution-treatment temperature of 550 °C was below the lower-temperature thermal event. For comparison, previously published melting ranges for AA6061 have been reported at approximately 580–652 °C, depending on alloy composition, initial material condition, and experimental methodology [19][20][21][22][23].

The observed thermal response provides a preliminary basis for identifying a processing-temperature window. However, the assignment of the thermal events and the extent of Mg–Si precipitate dissolution at 550 °C were not independently verified. Accordingly, the thermogram is presented as a thermal characterization result rather than direct evidence of complete precipitate dissolution or an optimized solution-treatment temperature.

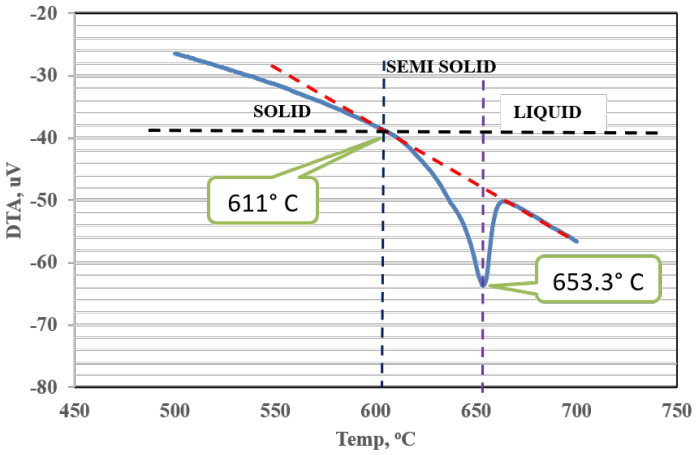

Fig. 4. Thermogravimetric and differential thermal analysis (TGA/DTA) response of the commercially sourced AA6061 aluminum alloy

3.2 Tensile Response After Artificial Aging

Figure 5 presents the tensile stress–elongation curves of the as-received (NHT) and artificially aged AA6061 specimens subjected to holding durations of 3, 5, and 7 h, originally identified as 150-3, 150-5, and 150-7, respectively. The curves exhibit differences in apparent ultimate tensile stress and horizontal extension among the investigated conditions. However, the strain definition, initial gauge length, and measurement procedure associated with the horizontal axis labeled "Elongation (%)" were not documented. Therefore, the horizontal extension of the curves cannot be directly interpreted as standardized elongation at fracture, and the apparent area beneath the curves cannot be reliably used to quantify tensile toughness.

Figure 6 summarizes the reported yield stress and elongation values for the investigated conditions. The as-received specimen exhibited a yield stress of 190.03 MPa, whereas the specimens aged for 3, 5, and 7 h exhibited values of 111.27, 129.01, and 126.53 MPa, respectively. Relative to the as-received condition, these values correspond to reductions of approximately 41.4%, 32.1%, and 33.4%. Among the aged conditions, the highest reported yield stress was obtained after 5 h of aging.

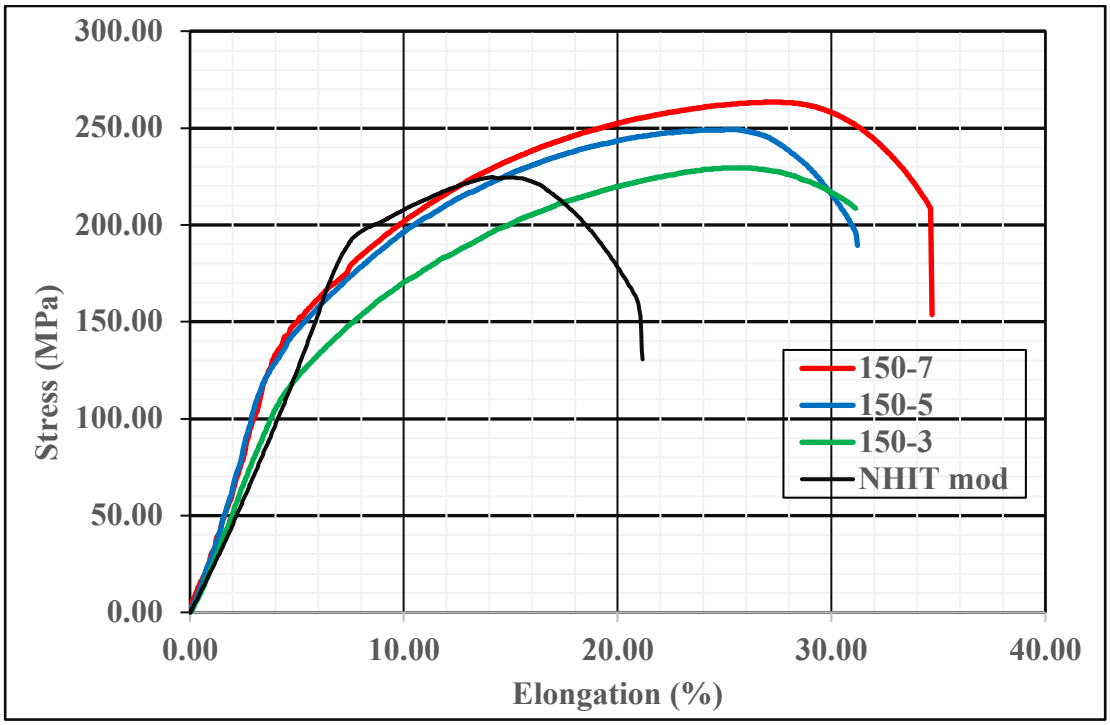

Fig. 5. Tensile stress–elongation curves of as-received and artificially aged AA6061 specimens under different aging durations

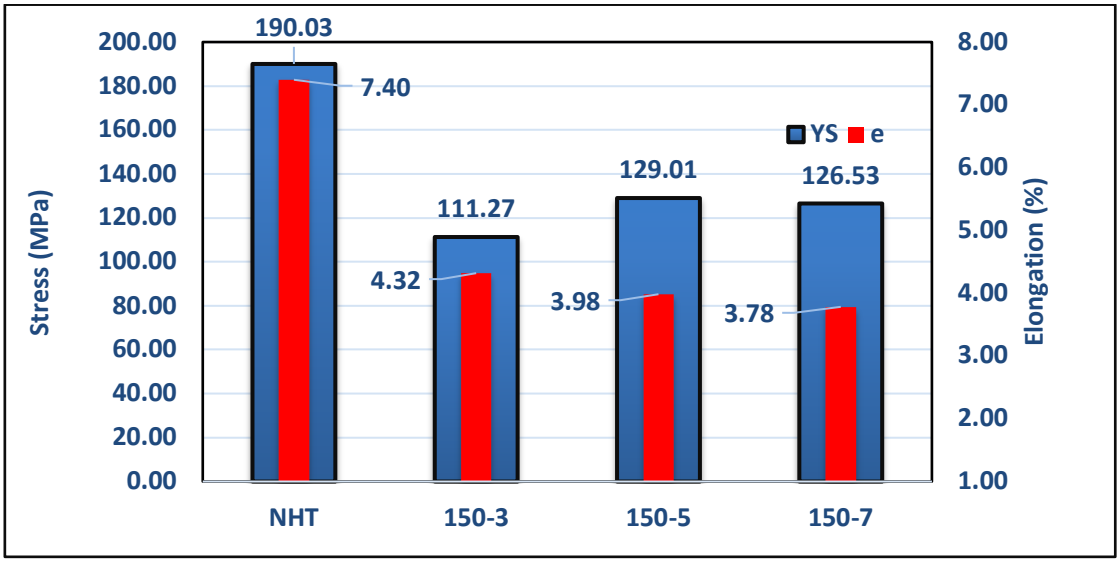

Fig. 6. Reported yield stress and elongation values of as-received and artificially aged AA6061 specimens

The corresponding elongation values reported in Figure 6 were 7.40%, 4.32%, 3.98%, and 3.78% for the as-received, 3 h, 5 h, and 7 h conditions, respectively. Although these values indicate a decreasing trend following heat treatment, they are inconsistent with the apparent horizontal extension of the curves in Figure 5. Consequently, the available results do not permit a definitive comparison of ductility among the treatment conditions until the original tensile measurements and elongation definitions are verified.

3.3 Bending Fatigue Life at Imposed Deflection Settings

Figure 7 presents the reported number of cycles to failure for the as-received and artificially aged AA6061 specimens tested under nominal imposed-deflection settings of 4°, 5°, and 6°. The fatigue-life response varied with both the imposed-deflection setting and the aging duration.

At the 4° setting, the as-received specimen exhibited the highest reported fatigue life of 5.625 × 10^6 cycles. The specimens aged for 3, 5, and 7 h reached 5.240 × 10^6, 5.350 × 10^6, and 5.415 × 10^6 cycles, respectively. Thus, none of the artificially aged conditions exceeded the as-received fatigue life at this setting.

At the 5° setting, the reported fatigue lives were 1.870 × 10^6, 1.635 × 10^6, 2.750 × 10^6, and 3.040 × 10^6 cycles for the as-received, 3 h, 5 h, and 7 h conditions, respectively. The 7 h condition exhibited the highest recorded fatigue life, corresponding to a relative increase of approximately 62.6% compared with the as-received condition, calculated as follows:

$$\Delta N = \frac{3.04-1.87}{1.87} \times 100\% = 62.6\% \quad (3)$$

At the 6° setting, the corresponding fatigue lives were 0.850 × 10^6, 0.510 × 10^6, 0.600 × 10^6, and 1.005 × 10^6 cycles. The 7 h condition again exhibited the highest recorded fatigue life, whereas the 3 h and 5 h conditions remained below the as-received value.

The reported fatigue-life ranking was not uniform across the three imposed-deflection settings. The as-received condition exhibited the longest recorded life at 4°, whereas the 7 h condition exhibited the longest recorded life at 5° and 6°. These comparisons describe the reported experimental values and do not establish statistical significance because specimen-level variability and replicate counts were not documented.

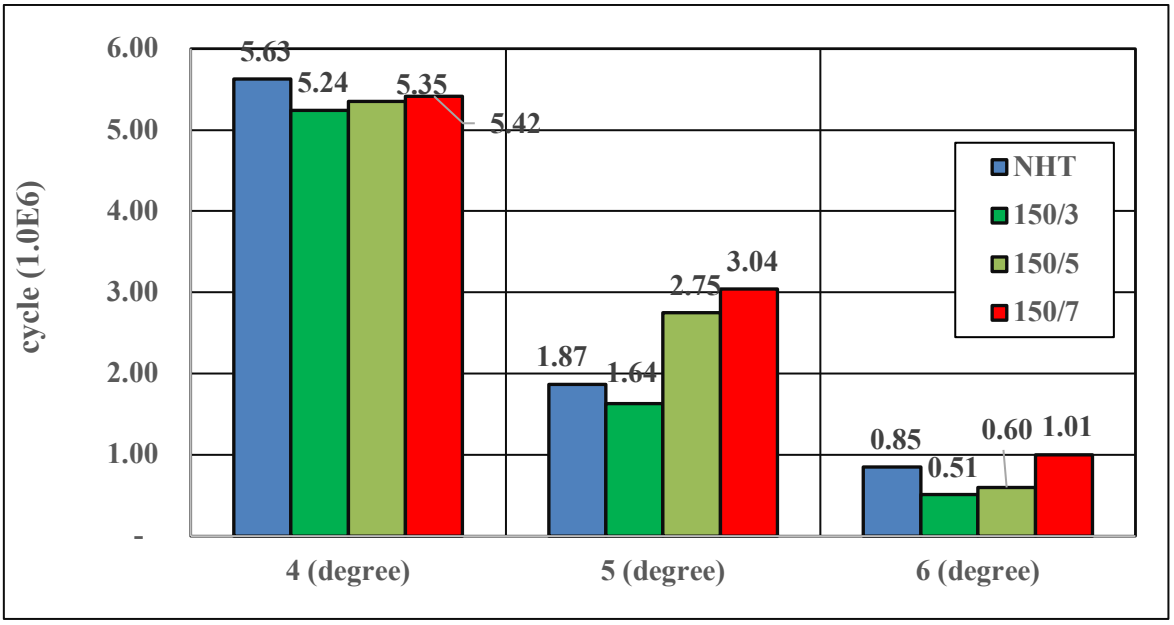

Fig. 7. Reported cycles to failure of as-received and artificially aged AA6061 specimens at nominal imposed-deflection settings of 4°, 5°, and 6°

3.4 Stress–Life Representation

Figure 8 presents the originally reported relationship between nominal bending stress and the number of cycles to failure. The plotted data indicate differences in the reported fatigue-life response across the investigated loading settings. However, the relationship between the imposed machine-angle or displacement settings and the corresponding bending-stress amplitudes was not documented sufficiently to reproduce the stress values presented on the vertical axis.

Consequently, the reported stress values in Figure 8 remain unverified, and the diagram cannot be considered a validated stress–life (S–N) relationship. The fatigue-life comparisons presented in Section 3.3 are therefore limited to the nominal imposed-deflection settings rather than equivalent stress amplitudes. Figure 8 is retained as part of the original experimental record pending verification of the bending-stress calculations and associated loading parameters.

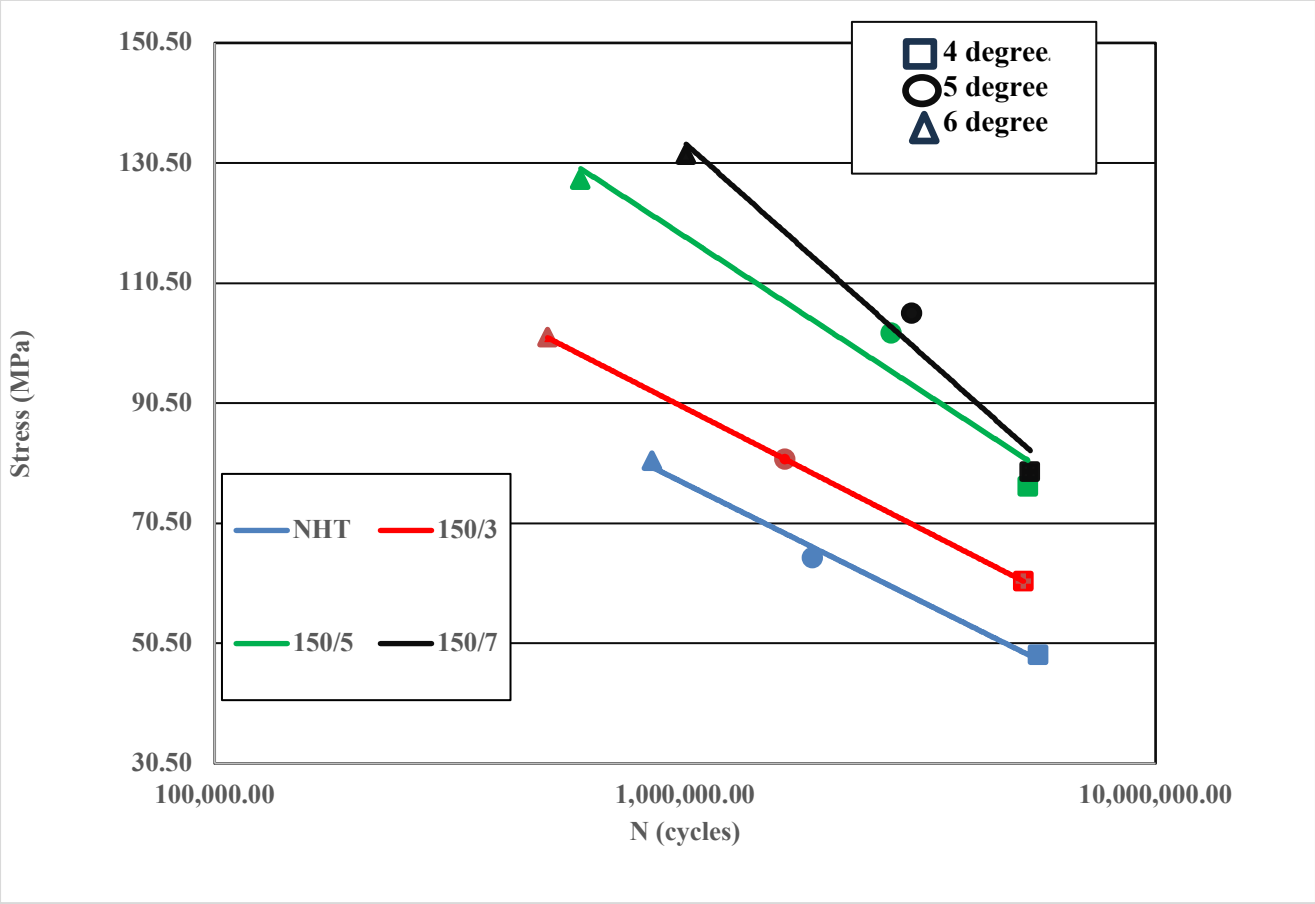

Fig. 8. Originally reported nominal stress–life representation of AA6061 specimens under different imposed-deflection settings (stress amplitudes not independently verified)

4. Discussion

4.1 Implications of Thermal-Analysis-Informed Solution Treatment

The selection of an appropriate solution-treatment temperature for AA6061 requires sufficient thermal energy to promote the dissolution of soluble strengthening phases while avoiding incipient melting and associated microstructural degradation. In the present study, the selected temperature of 550 °C was below the DTA thermal event identified near 611 °C, which was tentatively associated with the onset of melting. However, the empirical approach of selecting 90% of the melting-onset

temperature, particularly when calculated using the Celsius scale, does not constitute a thermodynamically valid criterion. Therefore, the selected temperature should be interpreted as an empirical processing condition informed by the observed thermal response rather than as a thermodynamically optimized solution-treatment temperature.

Previous investigations of solution treatment and precipitation behavior in aluminum alloys [24][4][16][23][25][26] provide a metallurgical basis for selecting temperatures that facilitate solute dissolution and subsequent precipitation during artificial aging. Nevertheless, the DTA response alone cannot establish the dissolution fraction of Mg–Si-containing precipitates or confirm the absence of localized incipient melting. Furthermore, the thermal event assigned to melting onset does not necessarily correspond to the solvus temperature governing precipitate dissolution. Consequently, the principal contribution of the thermal analysis in this study is to provide a material-specific screening observation for selecting the processing temperature, rather than direct evidence of an optimal solution-treatment window. Further microstructural characterization and independent thermal verification would be necessary to establish the relationship between the selected temperature, precipitate dissolution, and the resulting mechanical properties.

4.2 Strength–Ductility Trade-Off and Initial Material Condition

The tensile results reveal that the as-received AA6061 exhibited a higher yield strength (190.03 MPa) than the artificially aged specimens, which showed values ranging from 111.27 to 129.01 MPa. This reduction indicates that the applied solution-treatment and aging schedules did not restore the initial yield strength of the commercially supplied material. However, the observed response should not be interpreted solely as a consequence of artificial-aging duration because the initial temper, prior thermomechanical processing, and precipitation state of the as-received material were not independently established.

The mechanical response of precipitation-hardenable Al–Mg–Si alloys depends on the combined effects of dislocation density, solute distribution, and precipitate evolution during solution treatment, quenching, and aging [2][3][8][9][10][11][12][13]. Accordingly, several mechanisms may explain the lower yield strength after treatment. The as-received material may have possessed an initially strengthened temper or retained deformation-induced strengthening that was partially reduced during solution treatment. In addition, the subsequent aging schedule may not have generated a precipitate distribution sufficient to recover the original strengthening contribution. Variations in quenching rate, quench delay, natural aging before testing, grain structure, and specimen orientation may also have influenced the measured response. Because these factors were not independently characterized, attributing the reduction in yield strength specifically to precipitate coarsening, grain growth, or incomplete precipitation would be speculative.

The interpretation of ductility is further complicated by the inconsistency between Figures 5 and 6. Although the tensile curves in Figure 5 exhibit greater apparent horizontal extension for the aged specimens, Figure 6 reports a reduction in elongation from 7.40% in the as-received condition to 3.78% after 7 h of aging. These observations cannot be reconciled without confirming the strain definitions, initial gauge lengths, and elongation measurement procedures used to construct the respective figures. Therefore, the available results do not establish a definitive improvement in ductility following artificial aging. The specimens should also be described according to their documented solution-treatment and aging schedules rather than assigned a certified temper designation. Additional hardness measurements, differential scanning calorimetry, electron backscatter diffraction, and precipitate characterization would help clarify the mechanisms responsible for the observed strength–ductility response.

4.3 Fatigue Response and Nonuniform Ranking Across Deflection Levels

The bending-fatigue results demonstrate that the observed influence of artificial-aging duration depends on the imposed-deflection setting rather than following a uniform trend across all loading conditions. At the nominal 4° setting, the as-received material exhibited the longest fatigue life, reaching 5.625×10^6 cycles. In contrast, at the 5° setting, the specimen aged for 7 h reached 3.04×10^6 cycles, compared with 1.87×10^6 cycles for the as-received condition, representing a descriptive increase of approximately 62.6%. At the 6° setting, the 7 h condition also exceeded the as-received fatigue life, whereas the specimens aged for 3 and 5 h exhibited lower values. These findings indicate that the relative ranking of the treatment conditions changes with the imposed-deflection level.

Such differences are consistent with the complex relationship between static mechanical properties, cyclic deformation, crack initiation, and fatigue-crack propagation in aluminum alloys [14][15][27][28][29][30]. In precipitation-hardenable alloys, the characteristics of strengthening precipitates and the initial material condition may influence localized cyclic deformation and crack-development processes. However, the present experiments do not provide sufficient microstructural or fracture-surface evidence to establish which mechanisms govern the observed fatigue response. Consequently, the higher recorded fatigue life of the 7 h condition at selected settings should not be interpreted as direct evidence of superior intrinsic fatigue resistance.

An additional consideration is that the fatigue tests were conducted using nominal machine-angle settings corresponding to imposed displacements rather than independently verified stress amplitudes. Differences in specimen stiffness, local geometry, surface condition, and fixture compliance may influence the actual bending stresses experienced by individual specimens. Therefore, comparisons made at identical machine settings do not necessarily represent comparisons at identical stress amplitudes. Moreover, the absence of documented replicate counts and specimen-level variability prevents the determination of statistical significance. The reported fatigue-life differences should consequently be interpreted as descriptive experimental observations rather than statistically established treatment effects. A more definitive assessment would require repeated fatigue tests, validated stress calibration, controlled specimen preparation, and microstructural or fractographic characterization.

4.4 Study Limitations and Reproducibility

Several experimental limitations should be considered when interpreting the present findings. First, the actual chemical composition and initial temper of the commercially sourced AA6061 were not independently verified, limiting the assessment of the influence of the initial material condition. Second, as clarified in Section 2.3, the heat-treatment diagram (Figure 1) indicates 120 °C as the minimum artificial-aging temperature, whereas 150 °C represents the nominal aging temperature associated with the investigated specimens. These values therefore serve different purposes and should not be interpreted as conflicting experimental conditions. Nevertheless, verification of the actual furnace temperature using the original experimental records remains necessary to ensure the reproducibility of the heat-treatment schedule. Third, the elongation values presented in Figures 5 and 6 are inconsistent, requiring verification of the original tensile measurements and strain definitions before definitive conclusions regarding ductility can be established.

Furthermore, the available experimental records do not establish the number of independent specimens tested under each condition or provide sufficient information to calculate standard deviations, confidence intervals, or statistical significance. The fatigue-test documentation also lacks a validated relationship between imposed displacement and bending-stress amplitude, together with

complete information on loading frequency, stress ratio, and specimen-level variability. Additionally, the thermal events identified through thermal analysis and the proposed precipitation-related mechanisms were not independently confirmed through detailed thermal or microstructural characterization.

These limitations restrict the ability to establish definitive causal relationships between aging duration, precipitation evolution, tensile properties, and fatigue resistance. Nevertheless, the reported measurements provide a preliminary comparison of the mechanical responses of AA6061 specimens under the investigated processing and loading conditions. Future investigations should prioritize verification of the actual heat-treatment parameters, characterization of the initial material condition, consistent tensile-strain measurements, statistically replicated mechanical testing, and calibrated fatigue-stress evaluation to determine whether the observed treatment-dependent differences are reproducible.

5. Conclusions

For commercial AA6061 investigated under the reported conditions, thermal analysis identified a feature assigned to the onset of melting near 611 °C, and the authors selected 550 °C for solution treatment followed by water quenching and artificial aging for 3, 5, or 7 h. The thermal-analysis-based selection provides a material-specific starting point, although dissolution and incipient-melting boundaries were not independently confirmed.

The as-received specimen exhibited a yield stress of 190.03 MPa, higher than the 111.27–129.01 MPa range reported for the aged specimens. The stress–elongation plot suggests an increase in ultimate tensile response after aging, but the discordance between the elongation metrics in the two tensile figures prevents a definitive ductility ranking.

Fatigue life depended on imposed deflection. The as-received specimen reached the maximum at 4° (5.625×10^6 cycles), whereas aging for 7 h produced 3.04×10^6 cycles at 5°, compared with 1.87×10^6 cycles for the as-received condition (+62.6%). The aged conditions therefore did not show a uniform fatigue benefit across all three settings. Verification of aging temperature, loading calibration, and experimental repeatability is required before the findings can support a generalized process optimum.

Acknowledgement
The authors acknowledge Universitas Sriwijaya for providing facilities used in this research.

Conflict of Interest Statement
The authors declare no conflicts of interest that could have influenced the research or its presentation.

Author Contributions Statement
Faizal Safa: Conceptualization, Methodology, Supervision, Project administration, Writing – review & editing.
Nukman: Investigation, Formal analysis, Data curation, Validation, Visualization.
Irsyadi Yani: Formal analysis, Interpretation of results, Writing – original draft, Writing – review & editing.
All authors have read and approved the final version of the manuscript.

Data Availability Statement

Data underlying the figures are reported in the manuscript. Additional original experimental records should be made available by the corresponding author upon reasonable request, subject to their availability.

Ethics Statement

This research consists of laboratory characterization and mechanical testing of an aluminum alloy and does not report human or animal subjects. Any journal-specific ethics declaration should be completed in accordance with the actual research record.

References

[1] F. Czerwinski, "Thermal stability of aluminum alloys. Materials," *Materials,* vol. 13, no. 15, p. 3441., 2020.

[2] F. Ozturk, A. Sisman, S. Toros, S. Kilic and R. C. Picu, "Influence of aging treatment on mechanical properties of 6061 aluminum alloy," *Materials and Design,* vol. 31, p. 972–975, 2010.

[3] X. Fang, M. Song, K. Li and Y. Du, "Precipitation sequence of an aged Al-Mg-Si alloy.," *Journal of Mining and Metallurgy, Section B: Metallurgy,* vol. 46, no. 2, p. 171–180, 2010.

[4] M. . N. Amadoa and F. Daroquib, "Revision of the solvus limit of Al-Mg_2Si pseudo binary phase diagram," in *Procedia Materials Science*, 2015.

[5] T. Lever, P. Haines, J. Rouquerol, E. L. Charsley, P. V. Eckeren and D. J. Burlett, "ICTAC nomenclature of thermal analysis (IUPAC Recommendations 2014).," *Pure and Applied Chemistry,* vol. 86, no. 4, p. 545–553, 2014.

[6] I. Surya, Nukman, I. Yani, A. Arifin, K. Sahim and Saloma, "TGA/DTA analysis for AA6061 with fine coal blend.," in *AIP Conference Proceedings*, Palembang, 2023.

[7] M. Schoenitz, B. Patel, O. Agboh and E. L. Dreizin, "2010). Oxidation of aluminum powders at high heating rates.," *Thermochimica Acta,* no. 507-508, pp. 115-122, 2010.

[8] S. M. Rajaa, H. A. Abdulhadi, K. S. Jabur and G. R. Mohammed, "Aging time effects on the mechanical properties of Al 6061-T6 alloy," *Engineering, Technology & Applied Science Research,* vol. 8, no. 4, p. 3113–3115, 2018.

[9] G. Ay, M. O. Görtan and F. Ça˘gırankaya, "Effect of artificial aging conditions on mechanical properties of EN AW 6056 aluminum alloy.," *Metals,* vol. 16, no. 1, p. 88, 2026.

[10] R. N. Lumley, I. J. Polmear and A. J. Morton, "Interrupted aging and secondary precipitation in aluminium alloys," *Materials Science and Technology,* vol. 19, no. 11, pp. 1483-1490, 2003.

[11] J. Buha, R. N. Lumley and A. G. Crosky, "Microstructural development and mechanical properties of interrupted aged Al-Mg-Si-Cu alloy.," *Metallurgical and Materials Transactions A,* vol. 37, pp. 3119-3130, 2006.

[12] A. M. B. S. Antunes, C. A. R. P. Baptista, M. J. R. Barboza and A. L. M. Carvalho, "On the effect of interrupted ageing (T6I4) on the mechanical properties of AA6351 and AA7050 alloys.," *REM – International Engineering Journal,* vol. 74, no. 1, pp. 67-73, 2021.

[13] N. Y. Mahmood, A. A. Zainulabdeen, J. H. Mohammed and A. H. Oun, "Effect of cyclic heat treatment on microstructure and mechanical properties of AA 6061-T6 aluminum alloy," *Al-Nahrain Journal for Engineering Sciences,* vol. 23, no. 4, pp. 383-387, 2020.

[14] D. F. L. Nascimento, A. m. b. da Silva-Antunes, M. Paes and C. R. P. Baptista, C. A. R. P., "Low cycle fatigue behavior of Al-Mg-Si alloys extruded parts," *Materials Research,* vol. 25, no. e20220315, 2022.

[15] E. Georgantzia, P. J. Vardanega and M. M. Kashani, "Modelling low-cycle fatigue behaviour of structural aluminium alloys," *Bulletin of Earthquake Engineering,* vol. 23, pp. 1737-1758, 2025.

[16] W. Chae, M. Jeong, D. Lee, L. Lee, D. W. Chun, S. Y. Lee, S. K. Hong, S. H. Kim and J. H. Han, "Effects of pre/post-aging treatment on the mechanical properties and texture of asymmetrically rolled 6061 aluminum alloy: Formability and planar anisotropy.," *Journal of Materials Research and Technology,* vol. 24, pp. 9476-9490, 2023.

[17] Y. J. Sheng, H. T. Qing, Y. Jie, Y. W. Chun, F. S. Hao, L. R. Run, R. S. Hao and N. Guan, "Microstructural characterization and mechanical properties of 6061 aluminum alloy processed with short-time solid solution and aging treatment," *Journal of Alloys and Compounds,* vol. 960, no. 170704, 2023.

[18] Z. Zhang, S. H. Kang, Y. Y. Kim, K. Euh, Y. H. Cho and H. W. Son, "Effect of Ag and Ge on the precipitation behavior and resultant properties of AA6061 alloys," *Journal of Materials Research and Technology,* vol. 28, pp. 1330-1340, 2024.

[19] H. C. Tran, D. K. Huynh, M. U. Albab and M. A. Nguyen, "A multiscale simulation framework for predicting the hot cracking behavior of aluminum 6061 during laser welding," *Optics and Laser Technology,* vol. 192, no. 113719, 2025.

[20] E. Becker and A. Neag, "Aluminiums for thixoforging and preparatory conditions and parameters necessary before forming: A review," *Heliyon,* vol. 9, no. 12, 2025.

[21] J. W. Bray, "Aluminum Mill and Engineered Wrought Products," in *ASM Handbook*, vol. 02, ASM International, 1990, pp. 137, 181.

[22] L. Xiong, Y. Wang, C. Chen, M. Chang, D. Feng, Y. Guo and S. Zhao, "Effects of compression and isothermal treatment parameters on the microstructures and textures of semi-solid 6061 aluminum alloy prepared by SIMA process," *Journal of Alloys and Compounds,* vol. 1077, no. 189637, 2026.

[23] C. R. Brooks, "Heat Treating of Aluminum Alloys," in *ASM Handbook*, vol. 04, ASM International, 1991, p. 1873.

[24] L. Yong, F. Dongyu, B. Zhu, Y. Wan, S. Li and Y. Zhang, "Modeling of Isothermal Dissolution of Precipitates in a 6061 Aluminum Alloy Sheet during Solution Heat Treatment," *Metals,* vol. 11, no. 1234, 2021.

[25] T. He, S. W, S. Xiang, H. C and R. G. Ballinger, "Influence of aging on corrosion behaviour of the 6061 cast aluminium alloy," *Materials,* vol. 14, no. 8, p. 1821, 2021.

[26] S. S. Prathap, D. X. Tittu George, A. A. Joe Xavier and G. A. Raja, "Effect of heat treatment on the hardness behaviour of the aluminium 6061 alloy," 2023.

[27] K. Liu, F. A. Mirza and X. G. Chen, "Effect of overaging on the cyclic deformation behavior of an AA6061 aluminum alloy," *Metals,* vol. 8, no. 7, p. 528, 2018.

[28] J. C. Huang, C. S. Shin and S. L. I. Chan, "Effect of temper, specimen orientation and test temperature on tensile and fatigue properties of wrought and PM AA6061-alloys," *International Journal of Fatigue,* vol. 26, pp. 691-703, 2004.

[29] R. R. McCullough, J. B. Jordona, P. G. P.G. Allison, T. Rushing and L. Garcia, "Fatigue crack nucleation and small crack growth in an extruded 6061 aluminum alloy," *International Journal of Fatigue,* vol. 119, p. 52–61, 2019.

[30] H. Yang, F. Qin, Y. Cui, T. Lin and Y. Zheng, "Precipitation-controlled fatigue crack propagation mechanism combined with texture and SF-KAM synergy effect in forged aluminum alloy wheels," *Materials Science & Engineering A,* vol. 959, no. 150021, pp. 1-29, 2026.